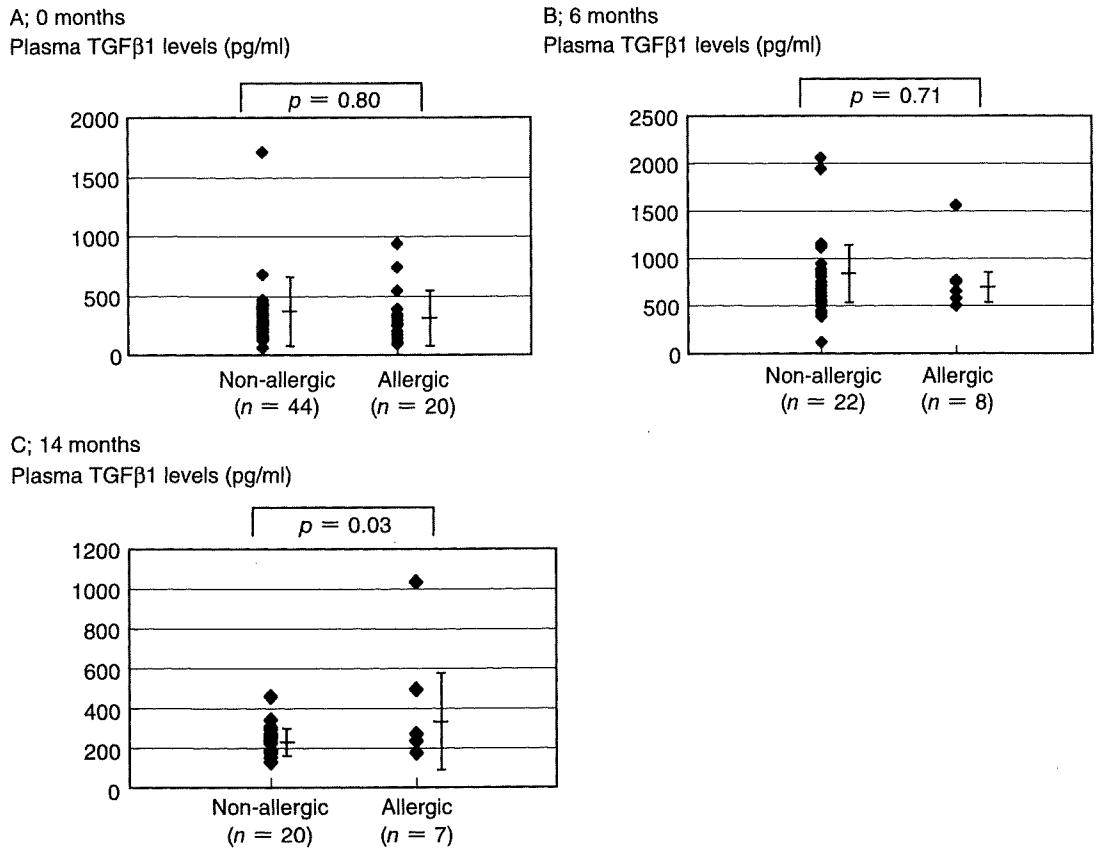

Fig. 2 Plasma TGFβ1 levels of non-allergic and allergic subjects at 0 months (**A**), 6 months (**B**) and 14 months (**C**) are shown. The plasma TGFβ1 levels at 14 months of age in allergic subjects were significantly higher than those in non-allergic subjects ($p = 0.03$, **C**).

els were determined by using the Mann-Whitney unpaired U-test. Pearson's correlation coefficient was used for statistical analysis of plasma IgE levels and TGFβ1 levels. The chi-square test was performed for statistical analysis of allergic symptoms and C-509T within the TGFβ1 gene. Probability (p) values of less than 0.05 were considered to indicate statistical significance.

RESULTS

ALLERGIC DISORDERS AND SYMPTOMS IN SUBJECTS

By the age of 14 months, 20 of the 64 subjects were allergic and 44 were non-allergic as defined in the Methods. Of the 64 subjects, 19 had atopic dermatitis and 3 had bronchial asthma, while two subjects suffered from both atopic dermatitis and bronchial asthma. Peripheral blood samples were collected at 6 months of age in 30 subjects and at 14 months of age in 27 subjects.

CHANGES IN PLASMA TGF*β*1 LEVELS BY AGE

Plasma TGFβ1 levels at 0, 6, and 14 months of age are shown in Figure 1A. Plasma TGFβ1 levels were 306.2 ± 230.9 pg/ml (M ± SD) at 0 months ($n = 64$), 805.3 ± 428.4 pg/ml at 6 months ($n = 30$), and 273.6 ± 175.8 pg/ml at 14 months ($n = 27$). Plasma TGFβ1 levels at 6 months of age were significantly ($p < 0.0001$ for each) higher than those in both 0 months and 14 months.

TGFβ1 levels were measured at all 3 points in all 24 subjects (data shown in Fig. 1B). The plasma TGFβ1 levels at 6 months of age were significantly ($p < 0.0001$ for each) higher than at both 0 and 14 months. This pattern was observed in 22 of the 24 subjects whose plasma TGFβ1 levels were measured at all 3 points.

RELATIONSHIP BETWEEN PLASMA TGF*β*1 LEVELS AND ALLERGIC DISEASES OR PLASMA IgE LEVELS

Figure 2A, B, C show plasma TGFβ1 levels at 0, 6, and 14 months of age in non-allergic and allergic subjects. The plasma TGFβ1 levels at 14 months of age in allergic subjects were significantly higher than those in the non-allergic subjects ($p = 0.03$, Fig. 2C).

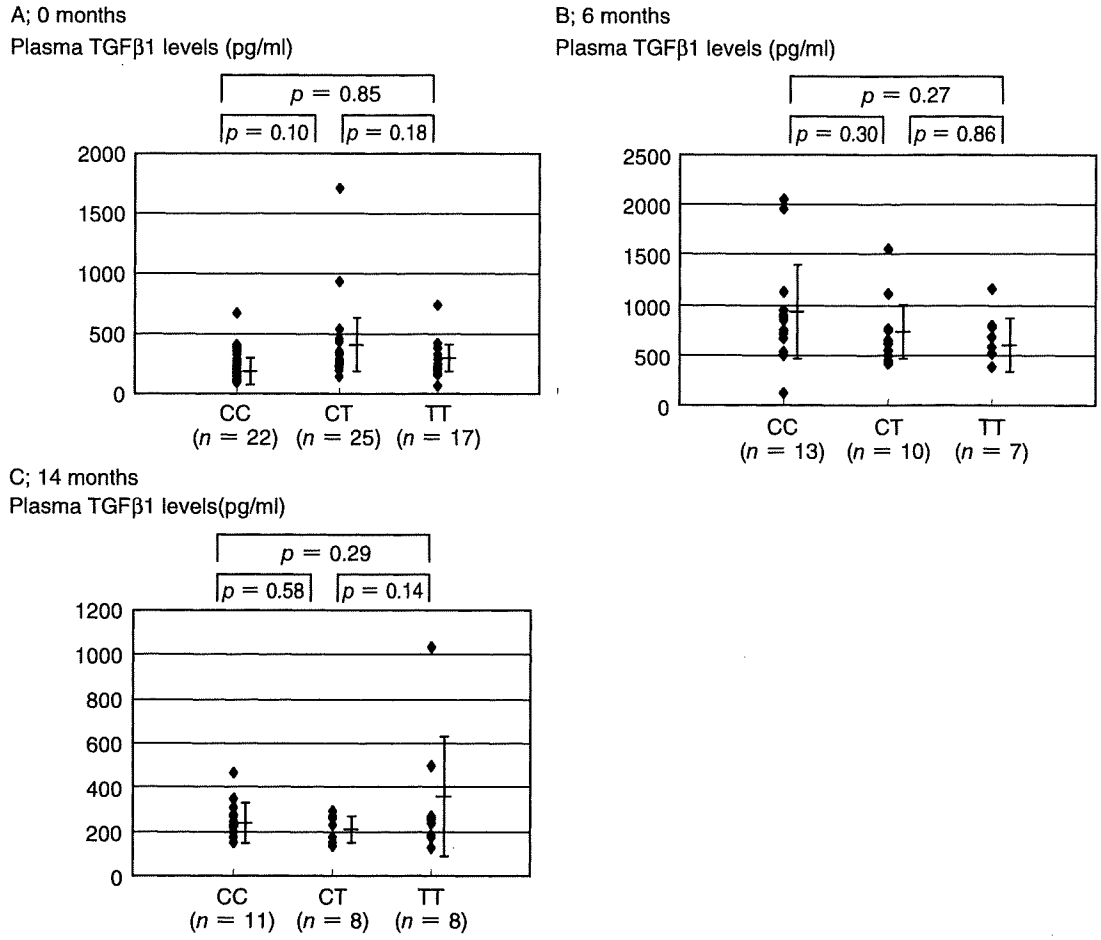

Fig. 3 Relationship between C-509T SNP of TGFβ1 gene and plasma TGFβ1 levels at 0 months (**A**), 6 months (**B**) and 14 months (**C**) is shown.

We also investigated the relationship between plasma IgE levels and TGFβ1 levels at 0, 6 and 14 months of age and found no significant relations (0 months; $p = 0.368$, 6 months; $p = 0.778$, 14 months; $p = 0.818$, data not shown).

PLASMA TGFβ1 LEVELS AND *TGFβ1* C-509T POLYMORPHISM

Among the 64 subjects, 22, 25 and 17 were classified as genotype CC, CT, and TT, respectively. As shown in Figure 3, these genotypes were not significantly related with plasma TGFβ1 levels at either 0, 6, or 14 months of age.

TGFβ1 C-509T POLYMORPHISM AND ALLERGIC DISEASES

The genotypes of *TGFβ1* C-509T polymorphism were not associated with the prevalence of atopic dermatitis at 6 months of age (Table 2) and 14 months of age (Table 3). However, the TT genotype was present in the TGFβ1 gene (C-509T) in all 3 patients with asthma at 14 months of age (Table 4). Furthermore, the TGFβ1 levels (M ± SD; 651.42 ± 544.79 pg/ml) in patients with asthma having the TT genotype in the TGFβ1 gene (C-509T) were higher than the TGFβ1 levels (M ± SD; 243.75 ± 89.19 pg/ml) in subjects without asthma (CC, CT or TT genotypes) at 14 months.

DISCUSSION

TGFβ1 is a multifunctional cytokine that has immunomodulatory effects produced by airway epithelial cells, eosinophils, helper T type 2 lymphocytes, macrophages, and fibroblasts. An important finding in this study is the changing pattern of plasma TGFβ1 levels over time at 0, 6, and 14 months of age. Plasma TGFβ1 levels at 6 months of age were the highest among these 3 measured age points. This pattern was observed in 22 of the 24 subjects whose plasma TGFβ1 levels were available at all 3 points. Statistically, the plasma TGFβ1 level at 6 months of age was significantly higher than that at 0 months and at 14

Table 2 Genotype frequency of C-509T *TGF-β1* promoter SNP in subjects with/without atopic dermatitis at 6 months

	CC	CT	TT	Total
Without atopic dermatitis	18	17	12	47 (74%)
With atopic dermatitis	4	8	5	17 (26%)
				($p = 0.551$)

Table 3 Genotype frequency of C-509T *TGF-β1* promoter SNP in subjects with/without atopic dermatitis at 14 months

	CC	CT	TT	Total
Without atopic dermatitis	18	19	12	49 (77%)
With atopic dermatitis	4	6	5	15 (23%)
				($p = 0.865$)

months of age ($p < 0.0001$ for each). We believe this is the first time this unique change in the plasma TGFβ1 level has been reported.

A previous study showed that the range of plasma TGFβ1 levels was 2000–4000 pg/ml in adult population.[5] In our study, the range of plasma TGFβ1 levels at 0, 6, and 14 months of age was 0–2500 pg/ml, and was lower than that of adult populations. At present, we do not know what causes the plasma TGFβ1 level changes, but one possible explanation could be that TGFβ1 is necessary for dramatic changes in immunological response or maturation at around 6 months of age. In other studies, the CD4 or CD8 cells producing cytokines, including TGFβ1, increased with age.[7,8] An increase in the number of TGFβ1- producing cells may partially explain why TGFβ1 production at 6 months was higher than that at 0 months. We are planning to observe further changes in plasma TGFβ1 levels from 14 months of age to 5 years of age or older.

We could not find any association of IgE with TGFβ1 in this study. TGFβ1 is produced by various cells including airway epithelial cells, eosinophils, lymphocytes, macropharges, and fibroblasts.[9,10] Various cell factors should be considered to evaluate the level of plasma TGFβ1.

It has been hypothesized that the T allele of the C-509T SNP enhances the Yin Yang 1 (YY1) transcription factor consensus binding site (-CCATCTC/TG-) on the TGFβ1 promoter and is responsible for increased TGFβ1 transcription.[11] In the present study there were no significant differences in plasma TGFβ1 levels at 0, 6, and 14 months of age regarding genotypes of *TGFβ1* C-509T. Pulleyn has shown that the T allele of the C-509T SNP is associated with the diagnosis of asthma and asthma severity.[12] In this study, only 3 subjects were given a diagnosis of bronchial asthma by the age of 14 months. Interestingly, the TT genotype was present in these 3 subjects (Table 4, $p = 0.016$). Although the prevalence of bronchial asthma at 14 months of age is low we need to obtain data at 5 years of age for an accurate evaluation of the role of the *TGFβ1* polymorphism in bronchial asthma. We are planning to increase the number of subjects to participate in future studies and to conduct a follow up for a longer time span.

Table 4 Genotype frequency of C-509T *TGF-β1* promoter SNP in subjects with/without bronchial asthma at 14 months

	CC	CT	TT	Total
Without bronchial asthma	22	25	14	61 (96%)
With bronchial asthma	0	0	3	3 (4%)
				($p = 0.016$)

In conclusion, this birth-cohort study suggests that plasma TGFβ1 levels are influenced by age and that the C-509T SNP of the TGFβ1 gene is an important susceptibility locus for asthma in infants at 14 months of age, despite the fact that the number of subjects who participated in this study was limited.

ACKNOWLEDGEMENTS

This study was supported by Health and Labour Science Research Grants for Research on Allergic Disease and Immunology from the Ministry of Health, Labour and Welfare.

REFERENCES

1. Shull MM, Ormsby I, Kier AB *et al.* Targeted disruption of the mouse transforming growth factor-beta 1 gene results in multifocal inflammatory disease. *Nature* 1992; **359**:693-9.
2. Duvernelle C, Freund V, Frossard N. Transforming growth factor-beta and its role in asthma. *Pulm Pharmacol Ther* 2003;**16**:181-96.
3. Redington AE, Madden J, Frew AJ *et al.* Transforming growth factor-β1 in asthma. Measurement in bronchoalveolar lavage fluid. *Am J Respir Crit Care Med* 1997;**156**: 642-7.
4. Li H, Romieu I, Wu H *et al.* Genetic polymorphisms in transforming growth factor beta-1 (TGFB1) and childhood asthma and atopy. *Hum Genet* 2007;**121**:529-38.
5. Meng J, Thongngarm T, Nakajima M *et al.* Association of transforming growth factor-β1 single nucleotide polymorphism C-509T with allergy and immunological activities. *Int Arch Allergy Immunol* 2005;**138**:151-60.
6. Ueda T, Niimi A, Matsumoto H *et al.* TGFB1 promoter polymorphism C-509T and pathophysiology of asthma. *J Allergy Clin Immunol* 2008;**121**:659-64.
7. Chipeta J, Komada Y, Zhang XL *et al.* CD4+ and CD8+ cell cytokine profiles in neonates, older children, and adults: increasing T helper type 1 and T cytotoxic type1 cell populations with age. *Cell Immunol* 1998;**183**:149-56.
8. Kawamoto N, Kaneko H, Takemura M *et al.* Age-related changes in intracellular cytokine profiles and Th2 dominance in allergic children. *Pediatr Allergy Immunol* 2006; **17**:125-33.
9. Kehrl JH, Roberts AB, Wakefield LM, Jakowlew S, Sporn MB, Fauci AS. Transforming growth factor beta is an important immunomodulatory protein for human B lympho-

cytes. *J Immunol* 1986;**137**:3855-60.
10. Alam R, Forsythe P, Stafford S, Fukuda Y. Transforming growth factor beta abrogates the effects of hematopoietins on eosinophils and induces their apoptosis. *J Exp Med* 1994;**179**:1041-5.
11. Silverman ES, Palmer LJ, Subramaniam V *et al.* Transforming growth factor-β1 promoter polymorphism C-509T is associated with asthma. *Am J Respir Crit Care Med* 2004;**169**:214-9.
12. Pulleyn LJ, Newton R, Adcock IM, Barnes PJ. TGF-β1 allele association with asthma severity. *Hum Genet* 2001; **109**:623-7.

Pediatrics International (2009) **51**, 107–109 doi: 10.1111/j.1442-200X.2008.02672.x

Original Article

Escherichia coli O-157-induced hemolytic uremic syndrome: Usefulness of SCWP score for the prediction of neurological complication

Takahide Teramoto, Toshiyuki Fukao, Kouichiro Hirayama, Tsutomu Asano, Yusuke Aoki and Naomi Kondo
Department of Pediatrics, Graduate School of Medicine, Gifu University, Yanagido, Gifu, Japan

Abstract ***Background***: Hemolytic uremic syndrome (HUS) is commonly caused by hemorrhagic colitis with Shiga toxin-producing *Escherichia coli* O-157. Central nervous system (CNS) involvements, including seizures, encephalopathy and brain infarction, are serious complications, but there are no useful scores for the prediction of CNS complications.
Methods: Routine laboratory data at onset of HUS were re-evaluated in 14 patients to find useful parameters for the prediction of CNS complication.
Results: Serum sodium and total protein were significantly lower and C-reactive protein (CRP) and white blood cell counts were significantly higher in patients with CNS complications than in patients without. A cumulated score, SCWP score (sodium, CRP, white blood cell count, and total protein) discriminated better between patients with/without CNS complications than individual values.
Conclusions: SCWP score would be useful for prediction of CNS complications

Key words children, *Escherichia coli* O-157, hemolytic uremic syndrome, prediction, SCWP score.

Hemorrhagic colitis caused by Shiga toxin-producing *Escherichia coli* O-157 is a major cause of hemolytic uremic syndrome (HUS), defined by the presence of microangiopathic hemolytic anemia, thrombocytopenia, and acute oligo/anuric renal failure.[1] Central nervous system (CNS) complications affect 20–50% of patients and often imply a poor prognosis with increased mortality and morbidity.[2–5] CNS pathology includes edema and infarction in the white matter, basal ganglia, and cerebellum. We recently encountered a 10-year-old O157-HUS patient with fulminant irreversible neurological sequelae. The aim of the present study was to predict CNS complication using routine laboratory data at the onset of O157-induced HUS.

Methods

Clinical records of 14 patients with O157-induced HUS who were admitted to Gifu University Hospital during 7 years were retrospectively analyzed. We divided these patients into five patients with neurological complications and nine patients without. Neurological complications include unconsciousness and/or convulsion. Evaluation and statistical analysis were performed using non-parametric Mann–Whitney *U*-test. Multivariate analysis was not performed because of the small sample size.

One patient (patient 1) developed multiple brain infarction 4 days after onset of bloody diarrhea and died. Another four patients with neurological complications were admitted with disturbed consciousness (Japan coma scale, II 10–III 300) and developed convulsions for a few minutes during hospitalization, but did not have significant abnormality on brain computed tomography and/or magnetic resonance imaging and recovered completely. Laboratory data at admission were used for the analysis.

Results

We re-evaluated routine laboratory data of patient 1 at admission. Her laboratory data, obtained at the onset of HUS, showed that the levels of blood urea nitrogen (BUN), serum creatinine, hemoglobin and platelet counts, did not deviate from the normal range (Table 1). In general, these data are considered as indicators of the degree of progression in HUS, because these reflect the degree of renal insufficiency, severity of hemolytic anemia and thrombocytopenia. In contrast, the levels of Na and total protein were low and the levels of C-reactive protein (CRP) and white blood cell (WBC) counts were high at the early stage of HUS.

We retrospectively evaluated routine laboratory data in 14 O157-HUS patients to determine which variables were significantly deviated at HUS onset in patients with neurological complications (Table 1). As shown Figure 1, serum creatinine, BUN, hemoglobin, and platelet count were not significantly different between patients with neurological complications and without. Serum Na and total protein, however, were significantly lower in patients with neurological complications than those without, and WBC and CRP were significantly higher in patients with neurological complications than those without. Hence these four variables

Correspondence: Takahide Teramoto, MD PhD, Department of Pediatrics, Graduate School of Medicine, Gifu University, 1-1 Yanagido, Gifu 501-1194, Japan. Email: t-tera@cc.gifu-u.ac.jp

Received 31 May 2007; revised 12 February 2008; accepted 25 March 2008; published online 3 September 2008.

Allergology International. 2008;57:367-376
DOI: 10.2332/allergolint.O-08-546

ORIGINAL ARTICLE

Expression, Purification and Structural Analysis of Human IL-18 Binding Protein: A Potent Therapeutic Molecule for Allergy

Takeshi Kimura[1,2], Zenichiro Kato[1,3,4], Hidenori Ohnishi[1], Hidehito Tochio[2,5], Masahiro Shirakawa[2,5] and Naomi Kondo[1,3,4]

ABSTRACT

Background: While interleukin-18 (IL-18) plays an important role in the innate and adaptive immune responses, it can also cause severe allergic inflammatory reactions. Thus it is a molecule currently being targeted for therapy. The natural intrinsic inhibitor of IL-18 receptor activation, IL-18 binding protein (IL-18BP), shows a great potential for the treatment of allergy.

Methods: Expression and purification of recombinant human IL-18BP (rhIL-18BP) were performed using the baculovirus system to develop a therapeutic molecule for the treatment of IL-18-related diseases and to investigate the structural basis of its inhibitory mechanism.

Results: Purified rhIL-18BP potently inhibited the production of interferon-gamma by peripheral blood mononuclear cells in the presence of lipopolysaccharide and by human myelomonocytic KG-1 cells in the presence of IL-18 (IC50 = 0.4 nM). Surface plasmon resonance showed a high affinity (Kd = 0.46 nM) for rhIL-18BP in binding hIL-18. Structural analysis indicated that the stoichiometry between IL-18 and IL-18BP is 1 : 1 in solution and the model structure of the complex suggests that the key residues on IL-18 (L5, K53, S55) and the estimated key residues on IL-18BP (F93,Y97, F104) could have interactions. The structural mechanism of IL-18BP inhibition might be a competition for Site 2 on rIL-18 so that IL-18BP can prevent IL-18 receptor alpha from binding to Site 2 and inhibit IL-18 receptor activation.

Conclusions: IL-18BP has unique features with respect to its structure, binding mode and inhibitory mechanism. It is a molecule that has a great potential for the therapy of allergy.

KEY WORDS

baculovirus, binding mode, IL-18 binding protein, purification, structure

INTRODUCTION

Interleukin-18 (IL-18) is a cytokine originally found to induce the production of interferon-gamma (IFN-γ) in T lymphocytes, and plays an important role in innate and adaptive immune systems.[1,2] To initiate the IL-18 pathway, the IL-18 receptor needs to be activated, which requires IL-18 receptor alpha (IL-18Rα, formerly known as IL-1Rrp) and IL-18 receptor beta (IL-18Rβ, formerly known as IL-1RAcPL) to heterodimerize.[2]

The structure of human IL-18 has been determined and it has shown that hIL-18 contains the β-trefoil fold that is similar to those found in interleukin-1 (IL-1) family members, making a new structural family in the interleukins.[3,4] Also, using mutant recombinant human IL-18 (rhIL-18) proteins in receptor-binding and cellular response assays, three important binding sites have been identified.[3] Two of these sites are important for binding to IL-18Rα, and the third is in-

[1]Department of Pediatrics, Graduate School of Medicine, [3]Center for Emerging Infectious Diseases (CEID), [4]Center for Advanced Drug Research (CADR), Gifu University, Gifu, [2]Department of Molecular Engineering, Graduate School of Engineering, Kyoto University, Kyoto and [5]CREST, Japan Science and Technology Agency, Saitama, Japan.
Correspondence: Zenichiro Kato, MD, PhD, Department of Pediatrics, Graduate School of Medicine, Gifu University, 1–1 Yanagido, Gifu 501–1194, Japan.
Email: zen-k@gifu-u.ac.jp
Received 22 February 2008. Accepted for publication 9 May 2008.

volved in cellular responses but not in IL-18Rα binding.[3]

By comparing the structure and the receptor binding sites of IL-18 with those of the IL-1 family members, a two-step ternary complex formation that involves IL-18, IL-18Rα, and IL-18Rβ has been revealed.[4] The formation of the ternary complex can then trigger a signal cascade that activates IL-1 receptor activating kinase (IRAK), tumor necrosis factor (TNF)-receptor associated factor 6 (TRAF6) and nuclear factor-kappa B (NF-κB).[5,6]

In medicine, the aberrant expression of IL-18 has been suggested to be responsible for several inflammatory conditions, such as allergies, autoimmune diseases, and neurological disorders.[2,7] Serum concentrations of IL-18 and IgE have been correlated with disease severity in atopic dermatitis (AD) patients.[7-9] In these patients, the serum concentration of IL-18 is significantly higher than that found in healthy individuals.[9] Furthermore, in response to lipopolysaccharide (LPS), leukocytes prepared from the peripheral blood of AD patients produced more IL-18 than the cells of healthy individuals.[7,8] In patients with bronchial asthma, the level of serum IL-18 is also elevated, and seems to correlate with disease severity.[7,10-14] As well, polymorphic genes for IL-18 and IL-18Rα have been found in association with allergy.[15-17] Collectively, these studies strongly suggest that IL-18 is responsible for causing and/or maintaining inflammatory conditions. Thus, IL-18 may be an ideal therapeutic target for the treatment of allergy.[7]

In clinical settings, humanized antibodies are widely used as therapeutic agents for the treatment of many diseases, including allergy.[18] Although anti-IL-18 antibody has been proven to be effective for preventing liver damage in mice, to date, there are no specific inhibitors against IL-18 to treat patients.[1,7,18] To this end, Hamasaki *et al.* recently reported a human anti-hIL-18 antibody (h18–108) that is capable of inhibiting IFN-γ production in a cell line.[19]

For therapeutic purposes, IL-18 binding protein (IL-18BP), a natural intrinsic inhibitor of hIL-18, may be an ideal candidate for use as a therapeutic agent.[20] One reason is that it is a natural inhibitor of IL-18, and its functional homologs have also been found in poxviruses, which utilize proteins to evade the immune system.[21-26] Also, the severity of autoimmune diseases appears to be influenced by the relative levels of IL-18 and IL-18BP.[27] Furthermore, IL-18BP has been shown to prevent disease development in various mouse models, which strongly supports IL-18BP's potential as a therapeutic agent.[28-30]

In this study, we performed high expression and purification of recombinant human IL-18BP (rhIL-18BP) using the baculovirus system to develop a therapeutic molecule for the treatment of IL-18-related diseases. A structural analysis of rhIL-18BP was performed to investigate the structural basis of its inhibitory mechanism.

METHODS

CONSTRUCTION OF EXPRESSION VECTOR FOR hIL-18BP

The IL-18BP isoform-a was selected from six isoforms of IL-18BP, because isoform-a most strongly inhibits IL-18 activity on human peripheral blood mononuclear cells (PBMCs) or human cell lines and has been widely used as the representative of the isoforms.[31,32] Total mRNA was extracted from the blood of a healthy volunteer, and single-stranded cDNAs were synthesized at 72℃ for 60 minutes using reverse transcriptase and oligo-dT primers. Only the coding region of the mature hIL-18BP isoform a (NM173042, residues 27–193 aa,) was amplified by PCR. The amplified fragment was cloned into T-vector (Invitrogen, USA), because the amino acid residues 1 to 26 of the hIL-18BP are recognized as a signal peptide in mammalian cells (Fig. 1A). One of the primers used in the PCR contained an *Eco*RI site and a signal peptide sequence for Sf9 insect cells, and by design, these were placed immediately upstream of the first codon of the mature hIL-18BP. The second primer contained the His-6 tag sequence, a stop codon, and a *Not*I site. The purified PCR product was subcloned into the pFastBac1 vector (Invitrogen, USA). The DNA sequence of the clone was confirmed by bi-directional sequencing. The construct was called pFastBac1-hIL-18BP-His6 (Fig. 1B).

PRODUCTION OF RECOMBINANT BACULOVIRUS

Generation of recombinant baculovirus expressing hIL-18BP in Sf9 cells was carried out with a Bac-to-Bac baculovirus expression kit (Invitrogen, USA). In accord with the manufacturer's protocol, pFastBac1-hIL-18BP-His6 was introduced into *E.coli* DH10Bac (Invitrogen, USA) for the transposition of IL-18BP into baculovirus genomic DNA (bacmid). Colonies containing the recombinant bacmid were isolated using a miniprep plasmid isolation kit (Promega, USA). The recombinant bacmid DNA was then used to transfect Sf9 cells, which were plated at a density of 1×10^6 cells per 35-mm well and then transfected with the bacmid DNA using Cellfectin reagent (Invitrogen, USA). The recombinant virus was harvested 72 hours post-transfection. Plaque assays were performed with the supernatants to determine the titer of recovered virion particles. Plaque assay and propagation of viruses were carried out according to the manual provided with the kit.

INSECT CELL CULTURE

Sf9 insect cells were cultured and routinely subcultured at 27℃. They were maintained either as a monolayer or as a suspension culture in Sf-900 II SFM (Invitrogen, USA) without antibiotics. Insect

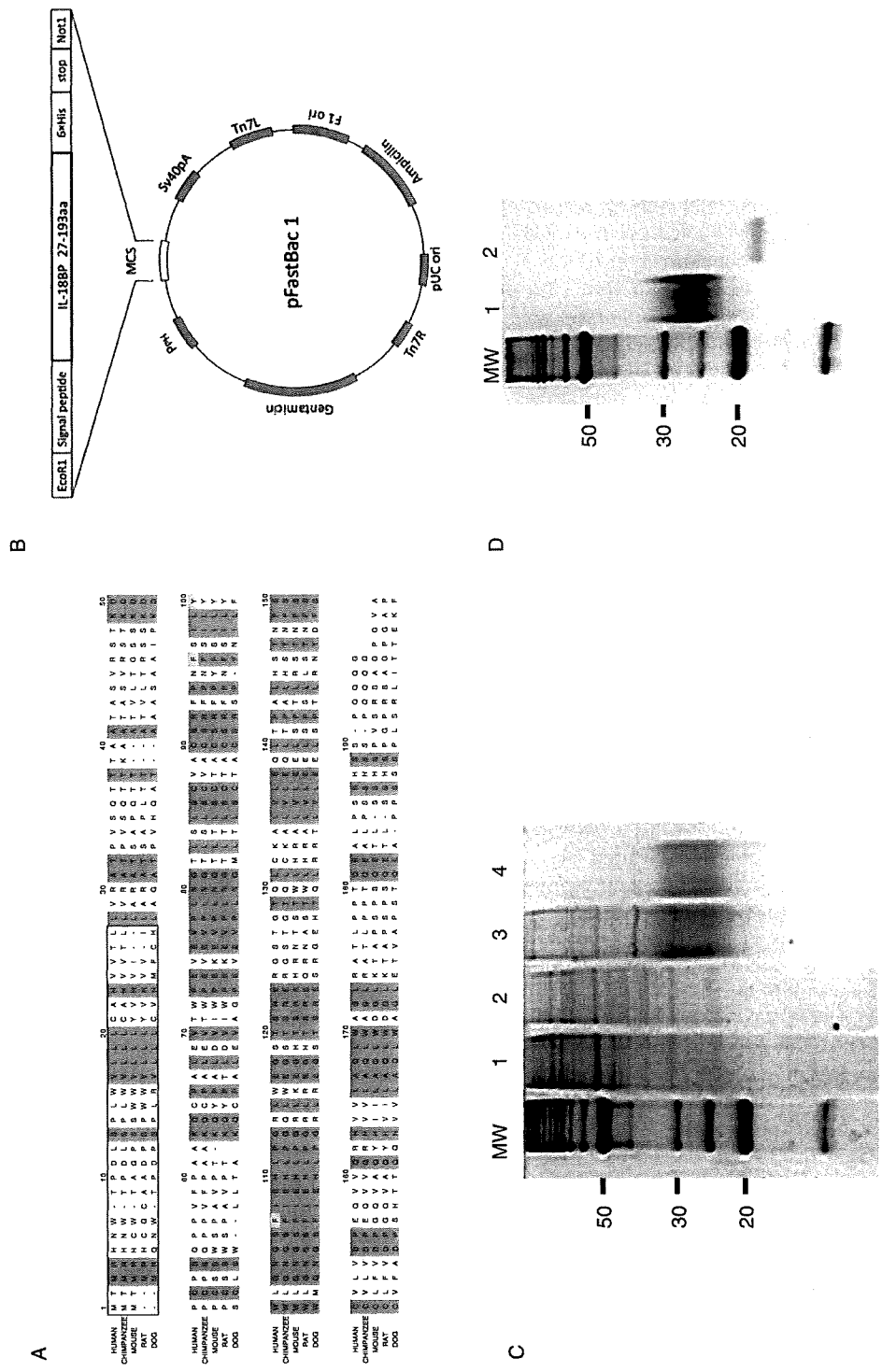

Fig. 1 Expression and purification of rhIL-18BP. **A**, Alignment for IL-18BPs. The signal peptide residues of the hIL-18BP in mammalian cells are boxed. Estimated key residues on hIL-18BP for hIL-18 binding are highlighted in yellow.[26] **B**, A map of the construct used for expression of hIL-18BP in the baculovirus system. **C**, Purification of rhIL-18BP. Lane 1: medium, lane 2: DEAE, lane 3: NiNTA, lane 4: Gel filtration. **D**, Deglycosylation by trifluoromethane sulfonic acid. Lane 1: before deglycosylation, lane 2: after deglycosylation.

cells in a monolayer culture were plated at a density of 1.0×10^6 cells/well in six-well plates. These cells were used to transfect recombinant bacmid DNA or for the determination of the optimal multiplicity of infection (MOI). The cells in the suspension culture were grown in a 25 ml volume of Sf-900 II SFM using 125 ml disposable Erlenmeyer flasks (Nalgene, USA). The flasks were maintained in a Bioshaker BR40LF (TAITEC, Japan) and were subjected to rotary shaking at a speed of 95 rpm (amplitude 35 mm). Stock

Sf9 cells that were grown in suspension were seeded at 0.5 × 10^6 cells/ml and culture passage was performed every 3 days during the log phase (4–6 × 10^6 cells/ml).

PURIFICATION OF hIL-18BP FROM BACULOVIRUS-INFECTED SF9 CELL CULTURE MEDIUM

For the purification of rhIL-18BP, Sf9 cells were subcultured in 1 L Fernbach flasks. Each flask received 400 ml of the cell culture at a concentration of 0.5 × 10^6 cells/ml. Shaking speed was set to 71 rpm (Amplitude 50 mm). When the subcultured cells reached a concentration of 2.0 × 10^6 cells/ml, Sf9 cells were infected with the recombinant baculovirus at an MOI of 0.1 plaque-forming units (pfu) per ml and were incubated for up to 72 hours.

Secreted rhIL-18BP was processed by centrifugation and filtration. Then, the medium was applied to a DEAE-Sepharose (GE health care, Sweden) open column (Bio-Rad, USA) equilibrated with buffer A (50 mM sodium-phosphate, pH 6.0 containing 50 mM NaCl). The flow through was concentrated 10-fold using a tangential flow filtration system; Masterflex L/S (Barnant Company, USA) and viva flow 50 (Vivasciece AG, Germany). This was then dialyzed against buffer B (50 mM Sodium Phosphate, 0.5 M NaCl, 10 mM Imidazol, pH 7.4) and insoluble material removed by centrifugation at 2 × 10^4 g; himac CR 20B2 (Hitachi, Japan). Dialyzed sample was loaded onto a Ni-agarose (GE Healthcare, Sweden) column equilibrated with buffer B. The column was then washed with buffer B and bound proteins were eluted by an elution buffer B with varying imidazol concentrations (50, 100, 200, 300 and 500 mM). The eluted fraction of rhIL-18BP was concentrated and further purified using a superdex75 16/60 (GE Healthcare, Sweden) size exclusion column equilibrated with 50 mM potassium phosphate buffer pH 7.0, containing 150 mM KCl and 0.1 mM EDTA. The purity of the preparation was assessed by SDS-PAGE.

DEGLYCOSYLATION OF rhIL-18BP BY TRIFLUOROMETHANE SULFONIC ACID

Deglycosylation was performed in a draft chamber (DF-19RST, DALTON, Japan). Freeze dried IL-18BP (30 μg) in glass vial and trifluoromethane sulfonic acid (TFMS) (Sigma Aldrich, Japan) was chilled on ice prior to mixing. Fifty micro liters of TFMS was added in a glass vial and gently mixed. The vial was then incubated for 50 hours on ice and neutralized with a solution of 500 μl of 1M-Tris. Neutralized rhIL-18BP was concentrated with a MicroconYM-10 (Millipore, USA) and dialyzed against 20 mM sodium phosphate buffer of pH 7.0 containing 150 mM NaCl before SDS-PAGE.

N-TERMINAL SEQUENCING BY EDMAN DEGRADATION

Purified proteins were electro-blotted onto a polyvinylidene difluoride membrane (Amersham Biosciences, UK) after SDS-PAGE for 1 hour at 200 mA in solution that contained 25 mM Tris, 192 mM glycine, and 10% methanol. The membrane was briefly stained with CBB R250 (Wako, Japan) and de-stained extensively in 45% and 90% methanol containing 7% acetic acid. The amino acid sequence analysis of the recombinant protein was carried out by an Edman degradation technique using a pulse liquid automatic sequencer (Model 491HT, Applied Biosystems, USA).

FUNCTIONAL ANALYSIS OF rhIL-18BP

Biological activity of rhIL-18BP was assayed by measuring its ability to inhibit the production of IFN-γ. This was performed as previously described with minor modifications.[17] Briefly, PBMCs were isolated from three volunteers and suspended at 1 × 10^6 /ml in the culture medium. PBMCs were cultured in the presence or absence of 1 ng/ml of the LPS with or without rhIL-18BP (400 ng/ml) for 24 hours at 37℃ in a humidified atmosphere containing 5% CO2. The cell culture supernatants were collected in test tubes, and the samples were spun to get rid of cells and then stored at −80℃ until assay. The concentration of IFN-γ was measured by enzyme-linked immunosorbent assay (ELISA), as previously described.[32]

MEASUREMENT OF rhIL-18BP-MEDIATED INHIBITION OF IFN-γ PRODUCTION IN KG-1 CELLS

In hIL-18 inhibition assay, the level of inhibition is determined by the amount of IFN-γ produced by the target cells. A detailed description has been reported.[32] Briefly, human myelomonocytic KG-1 cells (ATCC CCL246) were grown in RPMI1640 (Invitrogen, USA) supplemented with 10% heat-inactivated fetal calf serum (Sigma Aldrich, USA), L-glutamine (2 mmol/L) (Wako, Japan), penicillin (100 U/ml) (Meiji, Japan), and streptomycin (100 μg/ml) (Meiji, Japan). The rhIL-18 and rhIL-18BP prepared in our laboratory were mixed in the RPMI1640 medium noted above. The concentration of rhIL-18 was 4 ng/ml and rhIL-18BP was from 0 to 250 ng/ml. The mixed samples were incubated at 37℃ for 1 hour. Then, 100 μl of the mixture was added to the wells of a 96-well plate (Nunc, Denmark), which contained 100 μl of KG-1 cells (3 × 10^6 cells/ml) (The final concentration of rhIL-18 was 2 ng/ml and rhIL-18BP was from 0 to 125 ng/ml). The plate was further incubated at 37℃ for 24 hours in 5% CO2. The culture supernatants were collected, and the amount of IFN-γ produced by KG-1 cells was determined by ELISA.[32] IC50, the concentration of antagonists required to inhibit 50% of IFN-γ production by KG-1 cells stimulated with hIL-18, was then calculated.

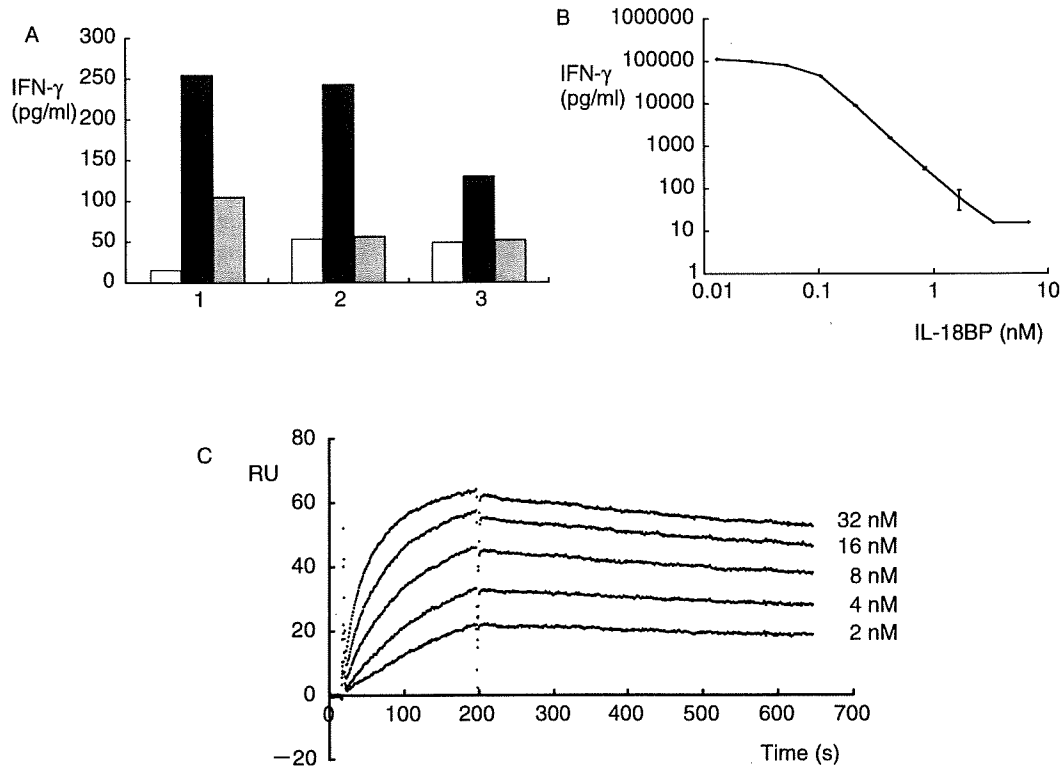

Fig. 2 Functional activity of purified rhIL-18BP. **A**, Inhibition of IFN-γ production by rhIL-18BP in LPS-stimulated human PBMCs. The numbers on the horizontal axis show the subject numbers. Open box, control; black box, LPS stimulation, grey box, LPS stimulation with rhIL-18BP. **B**, Inhibition of IFN-γ production by a human cell line, KG-1. **C**, Dose-response of the rIL-18BP/rhIL-18 interaction by surface plasmon resonance (Kd = 0.46 nM).

MEASUREMENT OF rhIL-18BP'S BINDING ACTIVITY BY SURFACE PLASMON RESONANCE EXPERIMENT

In vitro affinity of the hIL-18 for rhIL-18BP was measured at 25℃ by surface plasmon resonance (SPR) using a BIAcore3000 (BIAcore, Sweden). A specific binding surface was prepared by coupling the anti-penta-His antibody (QIAGEN K.K, Japan) to a CM5 sensor chip by the standard amine coupling method, as recommended by BIAcore. Then, 6-his tagged rhIL-18BP was injected over the sensor chip and immobilized. The coupling density was limited to 120 resonance units (RU) . Samples of hIL-18 were diluted to varying concentrations ranging from 2 to 32 nM in HBS-EP buffer (10 mM HEPES, pH 7.4, 150 mM NaCl, 3.0 mM EDTA, 0.005% (v/v) surfactant P-20). For dissociation constant analysis, diluted hIL-18 samples were injected over the sensor chip at a flow rate of 20 μl/min. The sensor surface was regenerated by two 60-second pulses of 0.2 M glycine-HCl, pH 2.2. The sensorgrams obtained from various concentrations of rhIL-18 were fitted with BIAEVALUATION software (BIAcore, Sweden) in a 1-to-1 binding model.

ANALYTICAL GEL FILTRATION OF rhIL-18BP

The molecular mass of purified rhIL-18BP and the complex of rhIL-18 and rhIL-18BP were determined by size exclusion chromatography. A superdex200 10/30 GL column (GE Healthcare, Sweden) attached to a FPLC system (GE Healthcare, Sweden) was utilized and the study conducted at 4℃. The column was equilibrated with 50 mM potassium phosphate buffer of pH 7.0, containing 150 mM KCl and 0.1 mM EDTA. The column was calibrated with the following gel filtration standards (Bio-Rad Laboratories, USA): thyroglobulin (670 kDa), bovine γ-globulin (158 kDa), chicken ovalbumin (44 kDa), equine myoglobin (17 kDa), and vitamin B_{12} (1.35 kDa) at a flow rate of 0.25 ml/min. Samples with only hIL-18BP, only rhIL-18 or a mixture of rhIL-18BP and rhIL-18 at a 1 : 2 ratio were used for the analysis. Protein elution was monitored and detected by UV absorption at 280 nm. We plotted the logarithm of the molecular weight versus the elution volume, and calculated the correlation line. The elution volume of rhIL-18BP and the complex of rhIL-18/rhIL-18BP were plotted and the deduced molecular weight determined.

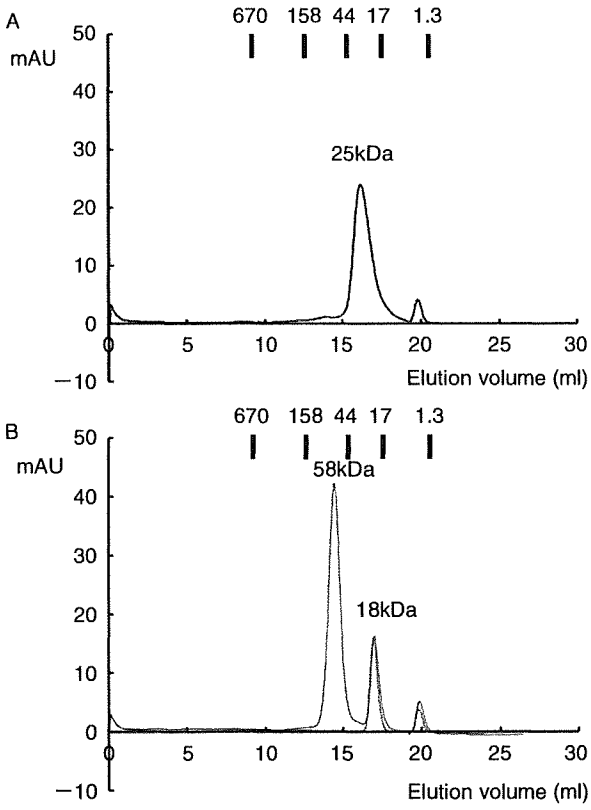

Fig. 3 Stoichiometric analysis of the rhIL-18/rhIL-18BP complex. **A**, Gel filtration of rhIL-18BP. **B**, Gel filtration of the rhIL-18BP/rhIL-18 complex. A solid line indicates the sample that contained a mixture of rhIL-18BP and rhIL-18 at 1 : 2 ratio, a dashed line, indicates the sample with only rhIL-18.

HOMOLOGY MODELING OF THE STRUCTURES

The sequence alignment of IL-18BP from different species was performed using ClustalW (http://www2.ebi.ac.uk/clustalw/) with a BLOSUM matrix. Homology modeling was performed using MOE software (CCG, Inc., Canada) with a combination of segment-matching and modeling of indels.[33,34] The templates used for the modeling were as follows: the NMR structure of hIL-18 (PDB: 1J0S) and the crystal structure of the domain 3 of hIL-1Rα (PDB: 1ITB) for the hIL-18: hIL-18BP complex; the NMR structure of hIL-18 (PDB: 1J0S) and the crystal structure of the hIL-10/anti-IL-10 Fab complex (PDB: 1LK3) for the hIL-18/human anti-hIL-18 Fab interaction. The modeled structures were refined by further energy minimization.

RESULTS

CHARACTERIZATION OF THE PURIFIED rhIL-18BP

High expressions of rhIL-18BP were obtained using the baculovirus expression system. We were able to obtain a yield of 2.5 mg/L of rhIL-18BP after Ni-NTA column purification (Fig. 1C). A further purification by gel filtration showed excellent purity and yielded 1.8 mg/L (Fig. 1C). To check the purity of the protein, electrophoresis was performed. Although the band appeared smeary, when we deglycosylated it with TFMS, a single sharp band of 18 kDa in size was detected (Fig. 1D). Edman degradation analysis of rhIL-18BP revealed the expected five N-terminal amino acid residues: (LVRAT). The sequence verified the identity of the expressed protein and indicated that the signal peptide from the vector was correctly cleaved at the N-terminal residue of mature rhIL-18 BP.

FUNCTIONAL ACTIVITY OF THE rhIL-18BP

The biological activity of rhIL-18BP was tested by measuring its ability to inhibit the production of IFN-γ by LPS-stimulated PBMCs from volunteers (Fig. 2A). The rhIL-18BP showed distinct inhibitory actions against IFN-γ production by PBMCs in response to LPS. rhIL-18BP only partly inhibited IFN-γ production by PBMCs from volunteer #1, while it almost completely inhibited those from volunteers #2 and #3 (Fig. 2A) . This diversity might be partly explained by the different amounts of IL-18 released from PBMCs of individual volunteers and/or in part by the different productions of other IFN-γ-related cytokines, such as IL-12 and IL-15.[8,17,35,36] As well, rhIL-18BP inhibited the production of IFN-γ by human KG-1 cells in the presence of IL-18 (IC50 = 0.4 nM, Fig. 2B).

His-tagged rhIL-18BP was immobilized on a BIAcore sensor chip coated with anti-His-tag antibodies and its binding activity monitored in real time with a BIAcore 3000 sensor. A sensorgram of rhIL-18 showed a rapid increase in signal during the association phase and a slow decline in the dissociation phase (Fig. 2C), demonstrating a fast on-rate and a slow off-rate. The estimated Kd of 0.46 nM was similar to results previously reported, indicating that the produced rhIL-18BP had proper structural folding.[25,26,31]

STRUCTURAL ANALYSIS OF rhIL-18BP

Gel filtration analysis revealed that rhIL-18BP is a monomer in solution (Fig. 3A) and that a complex of rhIL-18 and rhIL-18BP could be made in the same molar ratio (Fig. 3B). Together with the molecular weight of the complex, it is suggested that the complex could be made by one hIL-18 and one hIL-18BP (Fig. 3B).

Based on the results of analytical gel filtration, a model structure of the rhIL-18/rhIL-18BP complex was constructed using the NMR structure of hIL-18 and the crystal structure of the domain 3 of IL-1Rα as templates[3] (Fig. 4). The analysis of the amino acid sequence alignment for IL-18BP revealed that the residues that are involved in the binding of hIL-18 are

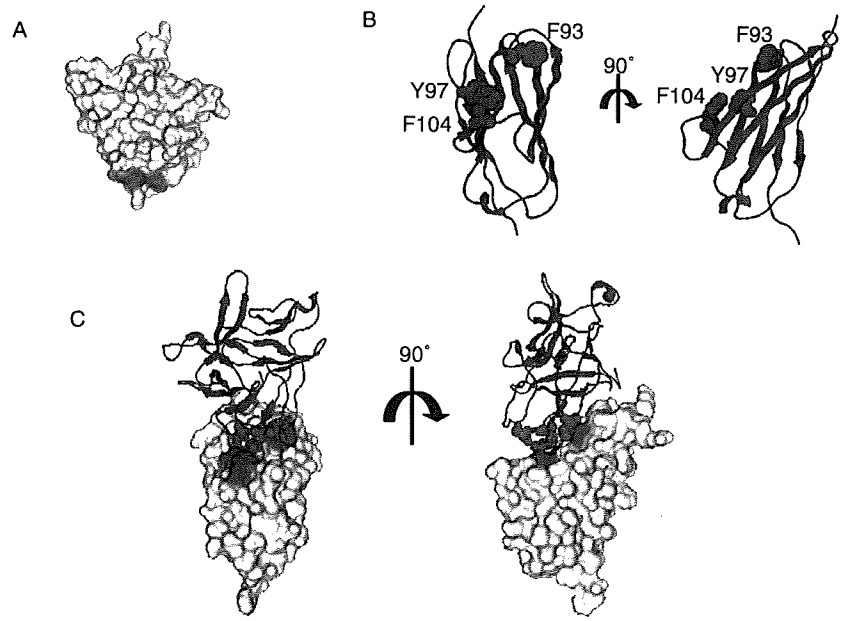

Fig. 4 A structural model of the hIL-18/hIL-18BP complex. **A**, Surface of hIL-18. Functional binding residues on hIL-18 for hIL-18BP are colored in orange. **B**, A structural model of the rhIL-18BP monomer. Estimated functional key residues of hIL-18BP for hIL-18 are shown as atoms in red. **C**, A model of the hIL-18/hIL-18BP complex (hIL-18 as a ribbon model, hIL-18BP as a surface representation, colored as in A or B).

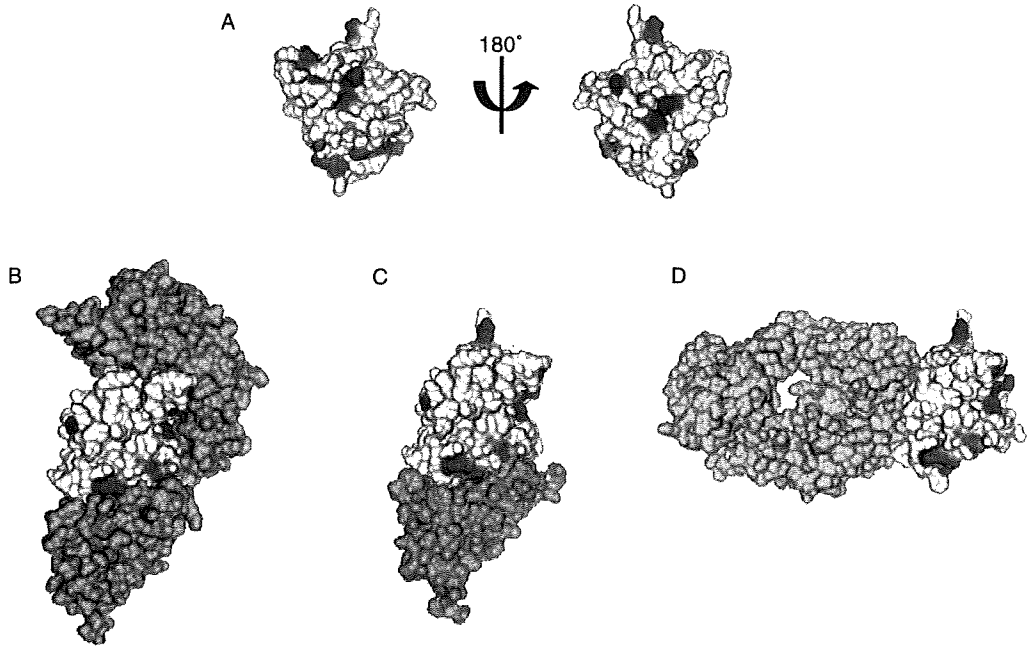

Fig. 5 Human IL-18 interacts differently with different proteins through its three binding sites. **A**, Receptor binding sites on hIL-18.[3] Sites 1, 2 and 3 are indicated in red, orange, and blue, respectively. **B, C, D,** Models of complexes between hIL-18 and hIL-18Rα (in grey), hIL-18BP (in yellow) and human Anti-hIL-18 Fab (in yellow).

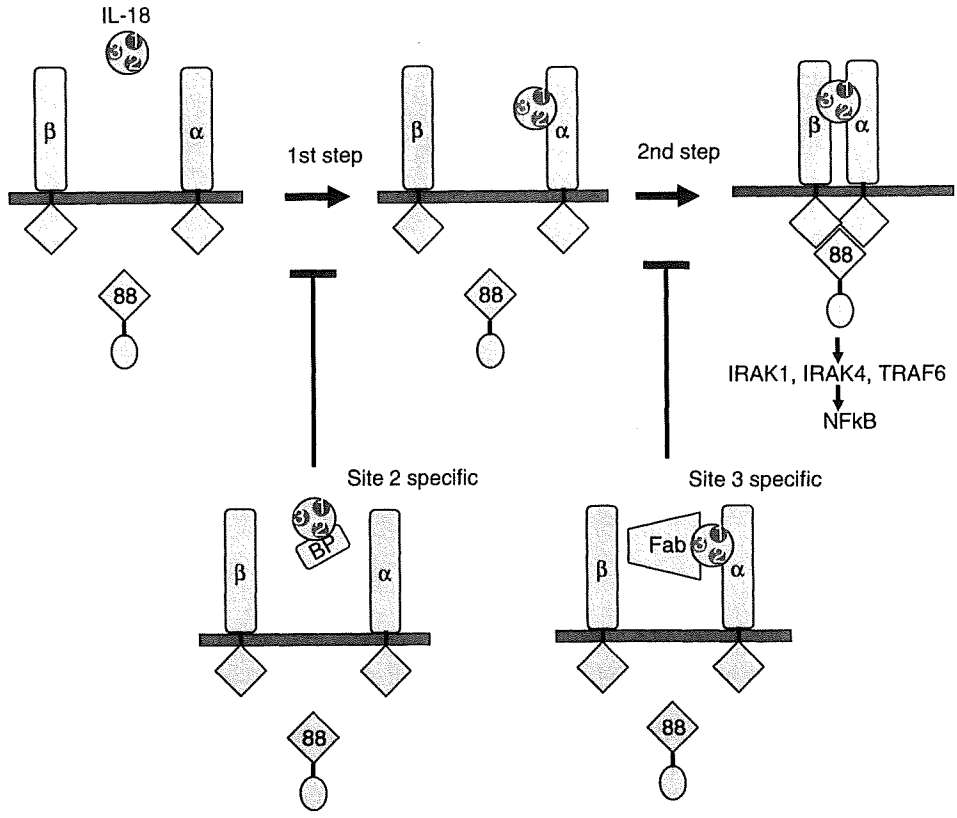

Fig. 6 A schematic model of IL-18 receptor activation and inhibition. A two-step complex formation model of IL-18 signaling is shown at the top. The inhibitory mode of IL-18BP or Fab fragment of h18－108 is shown at the bottom. Sites 1, 2 and 3 of hIL-18 are indicated in red, orange, and blue, respectively.

highly conserved between species[25,26] (Fig. 1A). Our model showed that the three key residues (F93, Y97, and F104) that are involved in binding IL-18 make hydrophobic patches that align with the binding interfaces of hIL-18 (Fig. 4C). The three key residues of hIL-18 for binding (L5, K53, and S55) have been shown to be involved in the interaction with hIL-18BP.[26]

DISCUSSION

Our previous structural analysis of the IL-18/IL-18 receptor interaction showed that there are 3 distinct and important binding sites on the surface of IL-18 (Fig. 5A).[3] Two of the sites (Sites 1 and 2) are responsible for binding to IL-18Rα while the third site is involved in binding to IL-18Rβ (Fig. 5A, B). Site 2 residue is also important for IL-18BP binding[3] (Fig. 5A, C). A recent study showed that a single-chain Fv (scFv) of an anti-human IL-18 antibody binds to Site 3 of IL-18 (Fig. 5A, D).[19] scFv (h18–108) showed a moderate binding affinity (Kd = 50 nM), whereas the Fab fragment of h18–108 showed a higher affinity (Kd = 3.7nM), suggesting that the stability of the binding surface structure could improve the affinity.[19] Further, hIL-18BP, which has a smaller molecular mass than scFv, showed a greater than 100-fold higher affinity (Kd = 0.46 nM)[25,26,31] than scFV. This suggested that the evolutionally improved structure of IL-18BP provided an optimal biding surface complementarity. Based on this, perhaps one could optimize the binding affinity of h18–108 by modifying the surface structure through *in vitro* mutagenesis or through a computational design, as it has been demonstrated for the anti-epidermal growth factor receptor drug, Cetuximab.[37]

IL-18 activates IL-18 receptor through a two-step binding mechanism as shown[3] in Figure 6. According to this model, the inhibitory mechanisms of IL-18BP and the Fab fragment of h18–108 antibody are different (Fig. 6). IL-18BP inhibits the receptor activation by competing for Site 2 on IL-18, which is also a binding site for IL-18Rα. On the other hand, the Fab fragment of h18–108 antibody binds to Site 3 on IL-18 to block IL-18 from binding to IL-18Rβ[3] (Fig. 6). The IC50 of IL-18BP has been shown to fall in the range of 0.04–0.46 nM, while it is 100 nM for the Fab frag-

ment.[19] This huge difference in IC50 may reflect the type of inhibitory mechanism that is employed (Fig. 6). Interestingly, an intact form of h18–108 antibody, an IgG molecule, has a much higher affinity with a Kd of 0.64 nM and an IC50 of 5 nM.[19] This improvement is most likely the result of its overall stability and the bivalency of the intact antibody molecule. Regardless of the affinity, these different molecules will be useful for determining the precise mechanism by which IL-18 receptor is activated or inhibited. Information gained from such studies will undoubtedly help us design potent therapeutic reagents.

A number of drugs targeting and neutralizing the deleterious effects of cytokines have been developed. Etanercept is a soluble fusion protein that is composed of two tumor necrosis factor alpha (TNF-α) receptors (p75) and a Fc fragment of a human IgG1 molecule; it has been shown to be effective and safe in patients with rheumatoid arthritis.[38] Recently, it was reported that the blockade of TNF-α by etanercept had efficacy in patients with asthma.[39,40] In addition to the anti-TNF drugs, the role of IL-18 in allergy suggests that drugs that neutralize the effect of IL-18, such as monoclonal antibodies or IL-18BP, may also be useful for the management of allergy.[7] The chemical characteristics of IL-18BP (a single polypeptide, a monomer, and with a low molecular weight of 25 kDa) support its use in clinical settings. Because of these characteristics, it is possible that its dosage could be lower than that of molecules, such as monoclonal antibodies and etanercept (multiple polypeptides, oligomer, high molecular weight of > 300 kDa) that are much bigger and more complex. Establishing a system that enables researchers to highly express the desired protein to study its structural mechanism could open avenues of research to develop new reagents and strategies for the treatment of various diseases, including allergy.

ACKNOWLEDGEMENTS

We thank W. Souma and K. Kasahara for technical help. This work was supported by the Research and Development Program for New Bioindustry Initiatives (2005–2009) of the Bio-oriented Technology Research Advancement Institution (BRAIN), by Grants-in-Aid for Scientific Research, and the National Project on Protein Structural and Functional Analyses from the Ministry of Education, Culture, Sports, Science and Technology-Japan.

REFERENCES

1. Okamura H, Tsutsi H, Komatsu T *et al.* Cloning of a new cytokine that induces IFN-gamma production by T cells. *Nature* 1995;**378**:88-91.
2. Nakanishi K, Yoshimoto T, Tsutsui H, Okamura H. Interleukin-18 is a unique cytokine that stimulates both Th1 and Th2 responses depending on its cytokine milieu. *Cytokine Growth Factor Rev* 2001;**12**:53-72.
3. Kato Z, Jee J, Shikano H *et al.* The structure and binding mode of interleukin-18. *Nat Struct Biol* 2003;**10**:966-71.
4. Kato Z, Kondo N. New methods for clinical proteomics in allergy. *Allergol Int* 2005;**54**:351-7.
5. Kojima H, Takeuchi M, Ohta T *et al.* Interleukin-18 activates the IRAK-TRAF6 pathway in mouse EL-4 cells. *Biochem Biophys Res Commun* 1998;**244**:183-6.
6. Robinson D, Shibuya K, Mui A *et al.* IGIF does not drive Th1 development but synergizes with IL-12 for interferon gamma production and activates IRAK and NFkappaB. *Immunity* 1997;**7**:571-81.
7. Tsutsui H, Yoshimoto T, Hayashi N, Mizutani H, Nakanishi K. Induction of allergic inflammation by interleukin-18 in experimental animal models. *Immunol Rev* 2004; **202**:115-38.
8. Shikano H, Kato Z, Kaneko H *et al.* IFN-gamma production in response to IL-18 or IL-12 stimulation by peripheral blood mononuclear cells of atopic patients. *Clin Exp Allergy* 2001;**31**:1263-70.
9. Ohnishi H, Kato Z, Watanabe M *et al.* Interleukin-18 is associated with the severity of atopic dermatitis. *Allergol Int* 2003;**52**:123-30.
10. El-Mezzein RE, Matsumoto T, Nomiyama H, Miike T. Increased secretion of IL-18 in vitro by peripheral blood mononuclear cells of patients with bronchial asthma and atopic dermatitis. *J Clin Immunol* 2001;**126**:193-8.
11. Yoshizawa Y, Nomaguchi H, Izaki S, Kitamura K. Serum cytokine levels in atopic dermatitis. *Clin Exp Dermatol* 2002;**27**:225-9.
12. Higashi N, Gesser B, Kawana S, Thestrup-Pedersen K. Expression of IL-18 mRNA and secretion of IL-18 are reduced in monocytes from patients with atopic dermatitis. *J Allergy Clin Immunol* 2001;**108**:607-14.
13. Wong CK, Ho CY, Ko FW *et al.* Proinflammatory cytokines (IL-17, IL-6, IL-18 and IL-12)and Th cytokines(IFN-g, IL-4, IL-10 and IL-13) in patients with allergic asthma. *Clin Exp Immunol* 2001;**125**:177-83.
14. Tanaka H, Miyazaki N, Oashi K *et al.* IL-18 might reflect disease activity in mild and moderate asthma exacerbation. *J Allergy Clin Immunol* 2001;**107**:331-6.
15. Higa S, Hirano T, Mayumi M *et al.* Association between interleukin-18 gene polymorphism 105A/C and asthma. *Clin Exp Allergy* 2003;**33**:1097-102.
16. Kruse S, Kuehr J, Moseler M *et al.* Polymorphisms in the IL-18 gene are associated with specific sensitization to common allergens and allergic rhinitis. *J Allergy Clin Immunol* 2003;**111**:117-22.
17. Watanabe M, Kaneko H, Shikano H *et al.* Predominant expression of 950delCAG of IL-18R alpha chain cDNA is associated with reduced IFN-gamma production and high serum IgE levels in atopic Japanese children. *J Allergy Clin Immunol* 2002;**109**:669-75.
18. Nowak D. Management of asthma with anti-immunoglobulin E: a review of clinical trials of omalizumab. *Respir Med* 2006;**100**:1907-17.
19. Hamasaki T, Hashiguchi S, Ito Y *et al.* Human anti-human IL-18 antibody recognizing the IL-18-binding site 3 with IL-18 signaling blocking activity. *J Biochem* 2005;**138**:433-42.
20. Novick D, Kim SH, Fantuzzi G, Reznikov LL, Dinarello CA, Rubinstein M. Interleukin-18 binding protein: a novel modulator of the Th1 cytokine response. *Immunity* 1999; **10**:127-36.
21. Born TL, Morrison LA, Esteban DJ *et al.* A poxvirus protein that binds to and inactivates IL-18, and inhibits NK cell response. *J Immunol* 2000;**164**:3246-54.

22. Calderara S, Xiang Y, Moss B. Orthopoxvirus IL-18 binding proteins: affinities and antagonist activities. *Virology* 2001;**279**:22-6.
23. Esteban DJ, Nuara AA, Buller RM. Interleukin-18 and glycosaminoglycan binding by a protein encoded by Variola virus. *J Gen Virol* 2004;**85**:1291-9.
24. Smith VP, Bryant NA, Alcami A. Ectromelia, vaccinia and cowpox viruses encode secreted interleukin-18-binding proteins. *J Gen Virol* 2000;**81**:1223-30.
25. Xiang Y, Moss B. IL-18 binding and inhibition of interferon gamma induction by human poxvirus-encoded proteins. *Proc Natl Acad Sci U S A* 1999;**96**:11537-42.
26. Meng X, Leman M, Xiang Y. Variola virus IL-18 binding protein interacts with three human IL-18 residues that are part of a binding site for human IL-18 receptor alpha subunit. *Virology* 2007;**358**:211-20.
27. Kawashima M, Yamamura M, Taniai M *et al.* Levels of interleukin-18 and its binding inhibitors in the blood circulation of patients with adult-onset Still's disease. *Arthritis Rheum* 2001;**44**:550-60.
28. Faggioni R, Cattley RC, Guo J *et al.* IL-18-binding protein protects against lipopolysaccharide-induced lethality and prevents the development of Fas/Fas ligand-mediated models of liver disease in mice. *J Immunol* 2001;**167**: 5913-20.
29. Banda NK, Vondracek A, Kraus D *et al.* Mechanisms of inhibition of collagen-induced arthritis by murine IL-18 binding protein. *J Immunol* 2003;**170**:2100-5.
30. Raeburn CD, Dinarello CA, Zimmerman MA *et al.* Neutralization of IL-18 attenuates lipopolysaccharide-induced myocardial dysfunction. *Am J Physiol Heart Circ Physiol* 2002;**283**:650-7.
31. Kim SH, Eisenstein M, Reznikov L *et al.* Structural requirements of six naturally occurring isoforms of the IL-18 binding protein to inhibit IL-18. *Proc Natl Acad Sci U S A* 2000;**97**:1190-5.
32. Matsukuma E, Kato Z, Omoya K *et al.* Development of fluorescence-linked immunosorbent assay for high throughput screening of interferon-gamma. *Allergol Int* 2006;**55**:49-54.
33. Levitt M. Accurate modeling of protein conformation by automatic segment matching. *J Mol Biol* 1992;**226**:507-33.
34. Fechteler T, Dengler U, Schomburg D. Prediction of protein three-dimensional structures in insertion and deletion regions: a procedure for searching data bases of representative protein fragments using geometric scoring criteria. *J Mol Biol* 1995;**253**:114-31.
35. Ong PY, Hamid QA, Travers JB *et al.* Decreased IL-15 may contribute to elevated IgE and acute inflammation in atopic dermatitis. *J Immunol* 2002;**168**:505-10.
36. Ethuin F, Gérard B, Benna JE *et al.* Human neutrophils produce interferon gamma upon stimulation by interleukin-12. *Lab Invest* 2004;**84**:1363-71.
37. Lippow SM, Wittrup KD, Tidor B. Computational design of antibody-affinity improvement beyond in vivo maturation. *Nat Biotechnol* 2007;**25**:1171-6.
38. Toussirot E, Wendling D. The use of TNF-alpha blocking agents in rheumatoid arthritis: an update. *Expert Opin Pharmacother* 2007;**8**:2089-107.
39. Brightling C, Berry M, Amrani Y. Targeting TNF-alpha: a novel therapeutic approach for asthma. *J Allergy Clin Immunol* 2008;**121**:5-10.
40. Kim J, Remick DG. Tumor necrosis factor inhibitors for the treatment of asthma. *Curr Allergy Asthma Rep* 2007;**7**: 151-6.

Theophylline-associated status epilepticus in an infant: pharmacokinetics and the risk of suppository use

Zenichiro Kato, Atsushi Yamagishi, Mitsuhiro Nakamura, Naomi Kondo
Gifu, Japan

Background: **Theophylline has been widely used to treat asthma, but recent studies have revealed that the possible risks for seizure may result in the revision of the therapeutic guidelines.**

Methods: **An 8-month-old boy who had been treated with oral sustained-release theophylline and additional aminophylline suppository was hospitalized. A combination of diazepam, lidocaine and thiopental was required to stop his convulsion.**

Results: **The pharmacokinetic study indicated that the usage of a sustained-release formula should not usually be over 15 mg/ml, but the additional use of an aminophylline suppository elevated the concentration to over 20 mg/ml and resulted in the severe adverse effects.**

Conclusion: **The parents of children and also physicians should be educated to ensure the proper use of the suppository formula.**

World J Pediatr 2009;5(4):316-318

Key words: **convulsion; pharmacokinetics; suppository; theophylline**

Introduction

Adverse neurological symptoms such as seizure during theophylline therapy are associated with the serum level of theophylline, a significant factor for increased morbidity.[1,2] We present a case of intoxication caused by add-on use of an aminophylline suppository during daily use of a sustained-release formulation. The pharmacokinetic study of this case suggests that the use of suppositories should be revised to avoid the possible adverse effects.

Case report

An 8-month-old boy who had been neurologically normal prior to this episode was transferred to our hospital due to status epilepticus. Before admission he was diagnosed as having bronchitis without fever and was treated with oral sustained-release theophylline (40 mg/day, 5.7 mg/kg per day) but without any antihistamines or antiallergic drugs at a local clinic. On the second day of illness, his mother gave him an aminophylline suppository (50 mg, 7 mg/kg), which had been previously provided by another clinic as a "cough stopper" to attenuate his coughing.

On admission, he was drowsy and his eyes were deviated and fixed to the left side, and he would respond only to painful stimuli. He had tachycardia (180/min) and tachypnea (50/min) without fever. He was diagnosed with a tonic convulsion, but not in a non-convulsive status epilepticus, and the initial dose of diazepam injection (2.5 mg, 0.35 mg/kg) slightly improved his tonic state. However, he developed a massive tonic seizure on the right arm and leg, which required three times of injections of diazepam (2.5 mg, 0.35 mg/kg), lidocaine (20 mg, 3.0 mg/kg) and thiopental (25 mg, 3.5 mg/kg) to cease the seizures. He showed right-sided paresis after the seizure, but the paresis diminished after several hours, suggesting Todd's paresis. No paroxysmal discharge was shown on electroencephalography, but there were periodic high voltage delta waves predominantly on the left hemisphere. Head computed tomography showed no abnormal lesion and he was discharged after three days of hospitalization without any neurological sequelae.

Laboratory tests showed the elevation of muscle related enzymes (aspartate amino transferase 66 mg/ml, lactate dehydrogenase 614 mg/ml, and creatine kinase 410 mg/ml) and abnormalities in a blood gas analysis

Author Affiliations: Department of Pediatrics, Graduate School of Medicine, Gifu University, Yanagido 1-1, Gifu 501-1194, Japan (Kato Z, Yamagishi A, Kondo N); Department of Pharmacy, Gifu University Hospital, Yanagido 1-1, Gifu 501-1194, Japan (Nakamura M)

Corresponding Author: Zenichiro Kato, MD, PhD, Department of Pediatrics, Graduate School of Medicine, Gifu University, Yanagido 1-1, Gifu 501-1194, Japan (Tel: +81 (58) 230 6386; Fax: +81 (58) 230 6387; Email: zen-k@gifu-u.ac.jp)

doi:10.1007/s12519-009-0061-y

Birth Defects Research (Part A) 00:000–000 (2009)

Case Report

Interstitial Deletion of 18q: Comparative Genomic Hybridization Array Analysis of 46, XX,del(18)(q21.2.q21.33)

AQ1

Zenichiro Kato,[1*] Wataru Morimoto,[1,2] Takeshi Kimura,[1] Akihiro Matsushima,[2] and Naomi Kondo[1]

[1]Department of Pediatrics, Graduate School of Medicine, Gifu University, Yanagido 1-1, Gifu 501-1194, Japan
[2]Division of Pediatrics, Nanao National Hospital, 3-1 Matsuhyakuyabe, Nanao 926-0841, Japan

Received 28 December 2008; Revised 20 August 2009; Accepted 21 August 2009

BACKGROUND: Interstitial deletion of chromosome 18q is rare, making it difficult to assign phenotypes to particular cytogenetic deletions. CASE: We present an 18-year-old female with an interstitial deletion of chromosome 18q21.2–q21.33. The clinical features included severe psychomotor retardation with mild growth retardation, hypotonia, midfacial hypoplasia, carp-shaped mouth, hypertelorism, strabismus, narrow upward slant palpebral fissures, short philtrum, everted lower lip, malformed ears, flat nasal bridge, and epicanthic folds. Brain abnormalities, such as agenesis of the corpus callosum, and abnormalities of the hands and feet were absent. Initially, the deletion was recognized as 18q21.1–q21.31 by conventional chromosomal analysis, and microarray-based comparative genomic hybridization revealed a 9.6-Mb deletion at 18q21.2–q21.33. The deletion included the transcription factor 4 gene and the methyl-CpG binding domain protein 2 (MBD2) gene, but not the MBD1 gene. CONCLUSIONS: The deletion of the transcription factor 4 gene suggested a possible contribution of the deletion to the patient's facial abnormalities, as observed in Pitt-Hopkins syndrome. Together with other reported cases with interstitial deletion of 18q, a possible contribution of haploinsufficiency in both MBD1 and 2 genes to a Rett syndrome-like phenotype was suggested, but further genetic studies on other cases are necessary to clarify the genotype-phenotype correlation. Birth Defects Research (Part A) 00:000–000, 2009. • 2009 Wiley-Liss, Inc.

Key words: interstitial deletion; 18q; transcription factor 4; methyl-Cog binding domain protein; comparative genomic hybridization

INTRODUCTION

Deletion of the long arm of 18q, 18q-, results in distinct clinical features, including mental retardation, hypotonia, and midfacial hypoplasia (Silverman et al., 1995). Many terminal deletion cases and proximal interstitial deletion cases have been described, but, to date, interstitial deletion within the distal portion of 18q has been reported only in three cases (Gustavsson et al., 1999; Wilson et al., 1979). We present here a further case with an interstitial deletion within the distal portion of 18q.

CASE REPORT

The patient, an 18-year-old female, is the second child of four siblings, born to healthy nonconsanguineous parents. The father and mother of the child at the time of birth were 28 and 26 years old, respectively.

*Correspondence to: Zenichiro Kato, Department of Pediatrics, Graduate School of Medicine, Gifu University, 1-1 Yanagido, Gifu 501-1194, Japan.
E-mail: zen-k@gifu-u.ac.jp
Published online 00 Month 2009 in Wiley InterScience (www.interscience.wiley.com).
DOI: 10.1002/bdra.20633

Thrombosis Research xxx (2009) xxx–xxx

Contents lists available at ScienceDirect

Thrombosis Research

journal homepage: www.elsevier.com/locate/thromres

Regular Article

A family having type 2B von Willebrand disease with an R1306W mutation: Severe thrombocytopenia leads to the normalization of high molecular weight multimers

Michio Ozeki [a,*], Shinji Kunishima [b], Kimiko Kasahara [a], Michinori Funato [a], Takahide Teramoto [a], Hideo Kaneko [a], Toshiyuki Fukao [a], Naomi Kondo [a]

[a] Department of Pediatrics, Gifu University Graduate School of Medicine, Gifu, Japan
[b] Department of Advanced Diagnosis, Clinical Research Center, National Hospital Organization Nagoya Medical Center, Nagoya, Japan

ARTICLE INFO

Article history:
Received 8 March 2009
Received in revised form 9 August 2009
Accepted 10 August 2009
Available online xxxx

Keywords:
type 2B von Willebrand disease
von Willebrand factor
giant platelets
thrombocytopenia
polymorphism

ABSTRACT

In type 2B von Willebrand disease (2B VWD), abnormal von Willebrand factor (VWF) spontaneously binds to platelets. This leads to the clearance of the high molecular weight multimers (HMWM) of VWF and results in thrombocytopenia. Herein we report a family of 2B VWD with an R1306W mutation which caused thrombocytopenia with giant platelets. The most important finding in this study is dynamic changes in VWF values in association with platelet counts. When the proband (2 years of age) had severe thrombocytopenia, his HMWM were normal, however, hematological examination showed a low level of VWF and a lack of HMWM after platelet count recovered. His affected sister also exhibited similar phenomenona. These results suggest that the severe thrombocytopenia leads to decreased clearance of VWF HMWM and restoration of VWF HMWM in plasma. We must consider 2B VWD in the case of recurrent thrombocytopenia following infection or other stress condition.

Introduction

Von Willebrand disease (VWD) is a common heterogeneous bleeding disorder and is represented by a reduction and/or abnormal function of the von Willebrand factor (VWF) [1]. In type 1 and 3 VWD, deficiencies or the absence of the vWF protein are responsible for the bleeding syndrome. Type 2 VWD is characterized by a wide heterogeneity of functional and structural deficits. Type 2B VWD (2B VWD) is caused by the increasing binding affinity of VWF for platelet glycoprotein Ib (GPIb) and is characterized by the relative loss of VWF high molecular weight multimers (HMWM) in plasma [2]. Though patients with 2B VWD often have diverse symptoms, including moderate to severe thrombocytopenia, giant platelets and spontaneous platelet agglutination, the degree of these reported symptoms is highly variable [3]. Thrombocytopenia associated with 2B VWD is not a rare finding, especially in children [4]. It is found to be transient or persistent with variable platelet counts on different occasions. It is known that infusion of desmopressin (DDAVP) can induce the release of VWF from endothelial cells [5]. Other situations, such as physiological (pregnancy) or pathological (infections, surgeries) stress conditions, also induce the release of VWF in 2B VWD plasma [6,7]. These events are associated with the occurrence of thrombocytopenia and spontaneous platelet agglutination in 2B VWD. Saba et al. referred to 2B VWD patients with giant platelets, chronic thrombocytopenia and spontaneous platelet agglutination as type 2B Tampa [8].

The VWF gene, located on the short arm of chromosome 12 spans 178 kb in length and contains 52 exons. There is a pseudogene on chromosome 22 corresponding to VWF exons 23–34. These sequences have about 97% homology, which makes it difficult to detect mutations in these regions [9]. The gain of functional mutations in exon 28 of the VWF gene encoding the VWF A1 domain is reported to be responsible for 2B VWD.

Herein we present a family of type 2B VWD with an R1306W mutation which caused severe thrombocytopenia with giant platelets. We describe the mutation analysis of this family and the dynamic changes in their platelet count, VWF and HMWM, which are useful for understanding the mechanism of the loss of VWF HMWM and severe thrombocytopenia in 2B VWD.

Patients

The proband

The proband was a 2-year-old Japanese boy who was admitted to our hospital due to presenting several purpura spots on the elbow following acute bronchitis. The patient's father had a past medical history of idiopathic thrombocytopenic purpura (ITP) during childhood. A hematological examination revealed thrombocytopenia (16,000/μl) measured by automated counter. PT was 83% (normal range: 70–120%), APTT was 45.0 s (normal range: 25.0–43.0 s) and

* Corresponding author. Department of Pediatrics, Gifu University Graduate School of Medicine, Yanagido 1-1, Gifu 501-1194, Japan. Tel.: +81 58 2306386; fax: +81 58 2306387.
E-mail address: mi_ti_ti_1227@yahoo.co.jp (M. Ozeki).

0049-3848/$ – see front matter ©2009 Elsevier Ltd. All rights reserved.
doi:10.1016/j.thromres.2009.08.012

International Journal of Pediatric Otorhinolaryngology 73 (2009) 1484–1487

Contents lists available at ScienceDirect

International Journal of Pediatric Otorhinolaryngology

journal homepage: www.elsevier.com/locate/ijporl

Case report

Congenital inner ear malformations without sensorineural hearing loss in children

Michio Ozeki[a,*], Zenichiro Kato[a,b,c,d], Hideo Sasai[a], Kazuo Kubota[a], Michinori Funato[a], Kenji Orii[a], Hideo Kaneko[a], Toshiyuki Fukao[a], Naomi Kondo[a,b,c]

[a] Department of Pediatrics, Graduate School of Medicine, Gifu University, 1-1 Yanagido, Gifu 501-1194, Japan
[b] Center for Emerging Infectious Diseases, Gifu University, 1-1 Yanagido, Gifu 501-1194, Japan
[c] Center for Advanced Drug Research, Gifu University, 1-1 Yanagido, Gifu 501-1194, Japan
[d] Molecular Cellular Biology, Harvard University, 7 Divinity Ave, Cambridge 02138, USA

ARTICLE INFO

Article history:
Received 28 June 2009
Accepted 16 July 2009

Keywords:
Inner ear malformation
Lateral semicircular canal (LSCC)
Sensorineural hearing loss (SNHL)
High-resolution computed tomography (HRCT)
High-resolution magnetic resonance (HRMR) imaging
Vestibular evoked myogenic potential (VEMP)

ABSTRACT

Inner ear malformations are frequently found in patients with congenital hearing loss. It has been reported that normal hearing is rare in patients with severe inner ear vestibular malformations. A 9-year-old boy had had complained of recurrent dizziness and disequilibrium for 2 months. Clinical and neuro-otological examinations showed peripheral involvement of the vestibular system, while audiological investigation was normal. High-resolution magnetic resonance imaging, with three-dimensional reconstruction, showed dysplasia of the bilateral lateral semicircular canals (LSCCs). Isolated vestibular malformation might not be as rare as previously thought, and should be examined by imaging of the temporal bone.

1. Introduction

Inner ear anomalies are frequently found in patients with sensorineural hearing loss (SNHL). In cases of posterior inner ear malformation, aplasia and/or dysplasia of the lateral semicircular canal (LSCC) are the most commonly encountered anomalies of the vestibular apparatus because LSCC is the last single structure to be formed during embryogenesis of the inner ear [1]. LSCC anomaly is thought to be common and usually associated with severe degrees of SNHL. However, the precise frequency of these anomalies is unknown because cases without symptoms are not detectable. Recently, new imaging diagnostic techniques such as high-resolution computed tomography (HRCT) and high-resolution magnetic resonance (HRMR) imaging have made it possible to diagnose minor inner deformities which were previously undetectable.

To the best of our knowledge, selective LSCC malformation with normal hearing has not been reported in children yet. We report a 9-year-old boy who had an isolated LSCC dysplasia without hearing loss and review the related previous reports.

2. Case report

A 9-year-old boy, complaining of recurrent dizziness and disequilibrium for 2 months, came to our hospital. He had had only one similar episode of sudden dizziness at school 4 months before.

Pure tone audiometry (Fig. 1A) and auditory brainstem response audiometry showed no definite abnormalities. Stabilography showed a worsening of sway with closed eyes. A subjective visual vertical (SVV) test showed normal. Voluntary eye movement showed a smooth and unimpeded pattern. The horizontal vestibulo-occular reflex (VOR) was present. No nystagmus was observed in the tests, including gaze, positional and positioning tests. Caloric stimulation with 20 ml of ice water elicited a reduced response in the right ear and no nystagmus in the left ear. The vestibular evoked myogenic potential (VEMP) was normal in the left ear. In the right ear, the P13 wave latency was prolonged and the P13-N23 interval was shortened (Fig. 1B). HRCT showed remarkable dysplasia of the LSCC in the right ear but mild dysplasia of the LSCC in the left ear (Fig. 2). Dilatation of the vestibule was indistinct. Both cochleas appeared almost normal in shape. The bilateral cochlear aqueducts

* Corresponding author. Tel.: +81 58 230 6386; fax: +81 58 230 6387.
E-mail address: mi_ti_ti_1227@yahoo.co.jp (M. Ozeki).

0165-5876/$ – see front matter © 2009 Elsevier Ireland Ltd. All rights reserved.
doi:10.1016/j.ijporl.2009.07.013

Brief Communication

Journal of Child Neurology
Volume 000 Number 00
Month 2009 1-3

10.1177/0883073809333535
http://jcn.sagepub.com
hosted at
http://online.sagepub.com

Oral Administration of the Thyrotropin-Releasing Hormone Analogue, Taltireline Hydrate, in Spinal Muscular Atrophy

Zenichiro Kato, MD, Miho Okuda, MD, Yu Okumura, MD, Takahiro Arai, MD, Takahide Teramoto, MD, Masaaki Nishimura, MD, Hideo Kaneko, MD, and Naomi Kondo, MD

Spinal muscular atrophy is an entity of neurodegenerative disorders at the anterior horn neuron of the spinal cord caused by telomeric survival motor neuron gene abnormality. There is no definitive treatment for spinal muscular atrophy, but recent reports have indicated the efficacy of intravenous injection, but not oral administration, of thyrotropin-releasing hormone. We treated an 18-year-old male patient with spinal muscular atrophy type III by oral administration of the thyrotropin-releasing hormone analogue, taltireline hydrate. His muscle strength increased significantly after the therapy, and he showed no clinical or laboratory identifiable adverse effects, including thyroid-stimulating hormone suppression that had been observed with intravenous thyrotropin-releasing hormone therapy. Oral administration of this thyrotropin-releasing hormone analogue should be noted as a promising therapy for spinal muscular atrophy.

Keywords: spinal muscular atrophy; thyrotropin-releasing hormone; oral administration

Spinal muscular atrophy is an entity of neurodegenerative disorders at the anterior horn neuron of the spinal cord caused by telomeric survival motor neuron gene abnormality.[1] However, the underlying mechanism between the genetic defect and the clinical symptom remains unclear, and there is no definitive treatment for spinal muscular atrophy. Recently, the efficacy of intravenous injection of thyrotropin-releasing hormone has been reported in spinal muscular atrophy[2,3] but not that of oral thyrotropin-releasing hormone analogues. Here, we report the efficacy and safety of an oral thyrotropin-releasing hormone analogue in the treatment of a patient with spinal muscular atrophy type III.

Received December 27, 2008. Received revised January 23, 2009. Accepted for publication January 23, 2009.

From the Department of Pediatrics, Graduate School of Medicine, Gifu University, Gifu, Japan.

The authors have no conflicts of interest to disclose with regard to this article.

Address correspondence to: Zenichiro Kato, Department of Pediatrics, Graduate School of Medicine, Gifu University, Yanagido 1-1, Gifu 501-1194, Japan; e-mail: zen-k@gifu-u.ac.jp.

Kato Z, Okuda M, Okumura Y, et al. Oral administration of the thyrotropin-releasing hormone analogue, taltireline hydrate, in spinal muscular atrophy. *J Child Neurol.* 2009;000:1-3.

Case Report

The patient, an 18-year-old male, showed normal motor development until he was 2.5 years old. He could walk at 15 months, but began to fall frequently while walking. Examinations including serum creatine kinase, head computed tomography (CT), and electroencephalogram (EEG) were normal at 2.5 years of age. At 4 years of age, the muscle conduction velocity was within the normal limits. However, at 5 years of age, fasciculation was obvious in his tongue and thumb, and the tendon reflexes of his extremities were reduced. He could stand up by himself but with Gowers' sign. At 6 years of age, an electromyogram (EMG) of his lower extremities showed neurogenic increased amplitude. Muscle biopsy showed irregular muscle atrophy with hypertrophic type I fibers and reinnervation. He was diagnosed as having spinal muscular dystrophy type III according to the clinical symptoms and laboratory findings. At 15 years of age, the genetic study revealed the homozygous deletion of exons 7 and 8 of telomeric survival motor neuron gene.

At 17 years of age, he was admitted to our hospital for intravenous thyrotropin-releasing hormone (protireline) therapy. Injection of thyrotropin-releasing hormone was performed according to the regimen reported by Tzeng et al.[3] The clinical study was approved by the ethical committee of our university, and the informed consents were obtained from the patient and the parents. He showed